# Chapter 1

# Introduction

## 1.1 Nonlinear dynamics and pattern formation

> *I am an old man now and when I will die and go to Heaven I hope that two things will be understood in the future. One is quantum electrodynamics and the other turbulent motion. With respect to the first, I am really rather optimistic.*
>
> (Said allegedly by the British Mathematican and Physicist Sir Horace Lamb, 1932.)

There are three directions in which physics pushes the limits to explore nature: towards the very large and fast, towards the very small, and towards the complex. With respect to the first two directions, one leaves the familiar space of the intermediate dimensions where our intuition is formed. Relativity and the uncertainty relation are two of the unexpected and counter-intuitive facts with which nature provided us.

Starting about thirty years ago, the third direction became more and more important and gave rise to a new field of physics: nonlinear dynamics, the study of nonlinear systems and equations. In this case one does not leave the familiar dimensions, and the underlying (classical) physical laws are well known. Nevertheless, also here one is lead to unexpected, often counter-intuitive, and therefore fascinating phenomena. The central role is played by the inherent nonlinearity of the systems, so that our basic concept of superposition cannot be applied. The system as a whole behaves differently from "the sum of its parts" [1]; qualitatively new phenomena emerge and its long-term behaviour may become unpredictable, even if the system is governed by deterministic equations.

This was already known by Poincaré [2] who showed that certain Hamiltonian systems cannot be separated into modes evolving independently from each other,

as is the case for any linear system. It took more than seventy years before the meteorologist Lorenz applied these ideas to dissipative systems. He showed that even a set of three ordinary differential equations, the so-called Lorenz model, can lead to irregular motion and to a sensitive dependence on the initial conditions. He coined the word "butterfly effect" meaning that even the motion of a single butterfly can influence the global evolution of the weather in the future.

Nowadays this behaviour is referred to as "deterministic chaos" [3] and, supported by the increase in computer power, the dynamics of low dimensional nonlinear systems (ordinary differential equations or iterated discrete maps) is fairly well understood. Typically, the behaviour depends on control parameters which, in the physical context, are external forces driving the system out of equilibrium. For low values the long-term behaviour of the system is stationary, described mathematically by an fixed point. Upon increasing the stress, many systems react with a cascade of increasingly complex states and eventually the dynamics is chaotic and is described by a fractal "strange attractor" [4]. There are at least three generic routes to chaos, the Ruelle–Takens route involving a few Hopf bifurcations [5], the intermittency route of Pomeau and Manneville [6] and the Feigenbaum scenario with an infinite cascade of period doublings [7]. Often it is even possible to reconstruct the attractor, or even the dynamics of a low-dimensional chaotic system, by measuring a time series of only one dynamical variable [8].

The next logical step towards complexity consists of the study of spatially extended nonlinear dissipative systems described by partial differential equations or high-dimensional discrete models. As in the low-dimensional case, typical systems are in an ordered (often featureless) state for low external stress. In reaction to an increasing control parameter, the systems develop spatially and spatio-temporally ordered structures, and eventually, spatio-temporal chaos or turbulence [9]. While to date little is known about these two "Holy Grails" of the field [9] we have an increasing number of analytical and numerical tools to investigate the spatio-temporal structures appearing spontaneously for an external stress higher than that for the unstructured state and lower than that for chaos, the domain of pattern formation [9, 10].

Patterns are ubiquitous in nature. Some examples are water waves driven by wind [11], cloud formations, sand dunes [12], the ripples appearing in stream beds and on dirt roads (the infamous "wash boards"), erosion structures, and snow flakes as well as other interfacial phenomena. Biological examples are population distributions [13], stripes and spots on animal coats [9, 14] or the (partially fractal) shape of fern leaves [15]. Geophysical examples include convection structures of the mantle of

the earth [16] or of the atmospheres of the large planets [17]. Other examples may lead to practical applications like modelling the stop-and-go waves of traffic flow on motorways [18], suppressing the spiral waves occurring in some heart deseases [19], or controlling chaos in general [8].

## 1.2 Hydrodynamic systems

For a quantitative understanding of pattern formation, one needs systems where (i) the basic equations describing the macroscopic dynamics are well established, and that (ii) allow reproducible precision experiments. The first point is best fulfilled for hydrodynamic systems. The second point restricts the investigations to rather few paradigmatic "standard" systems. It would be also useful to find general aspects not depending on particular systems. Such universal behaviour is typically found near the threshold to the first instability, so this range is particularly interesting.

The most prominent system of pattern formation is probably thermal convection in a simple fluid heated from below, known as Rayleigh–Bénard convection (RBC). RBC was investigated as early as 1900 [20, 21] and is the isotropic test system for natural phenomena such as cloud streets and convection phenomena in the mantle of the earth, but also for the transition to turbulence. For a review see Ref. [9] and the references therein. While the classic RBC predicts stationary patterns, variations like thermal convection in binary fluid mixtures [22], or in nematic liquid crystals [23, 24], show in some parameter ranges a bifurcation to oscillatory patterns (see also Chapter 5.6).

Another test system showing a rich scenario of patterns is the Taylor-Couette system where a fluid is confined to a gap between two concentric cylinders which rotate with different angular velocities [9]. In contrast to the buoyancy force of RBC, the instability is driven by centrifugal forces. From all systems, it is probably that system, whose basic equations (Navier–Stokes equations with no-slip boundary conditions) describe the dynamics most accurately.

The paradigma for anisotropic systems is electrohydrodynamic convection (EHC) in nematic liquid crystals (NLCs). The main advantages of EHC with respect to other systems are the convenient time scales in the experiments, many accessible control parameters, and the large aspect ratio (typically, of the order 1000), that can be realized experimentally. The main disadvantage of EHC are the complicated structure of the basic equations, the many (often unknown) material parameters, and the obviously incomplete standard hydrodynamic description. This last point is the motivation for most of the work in this thesis.

## 1.3 Electrohydrodynamic convection

### Nematic liquid crystals

The liquid-crystal state is sometimes called the fourth state of matter [25]. In fact, liquid crystals posses properties of both crystals and liquids. In nematic liquid crystals (nematics, NLC), considered exclusively in this work, the crystal-like properties come from the long-range uniaxial orientational order of the rod-like (or disc-like) molecules. The positional order of the centers of gravity of the molecules is short ranged which means, that the NLC can flow like a liquid.

I will consider the hydrodynamic description [26, 27, 25] which is based on local averages visualized by fluid elements. These fluid elements contain many individual molecules, so local averages can be introduced, but they are small enough to allow for a continuum treatment on the scale of the entire fluid.

The molecules of the NLC are not aligned perfectly. The degree of alignment is denoted by the scalar order parameter $S$ [25], and the locally-averaged orientation by the director field $\boldsymbol{n}$. Strictly speaking, $\boldsymbol{n}$ is not a vector, but it can be represented as an unit vector with an additional inversion symmetry (the molecular alignment does not distinguish right from left). While the order parameter can be assumed to remain constant for the phenomena studied in this work, the dynamics of the director field must be incorporated into a hydrodynamic description of a NLC.

The orientational order is associated with an orientational elasticity, i.e., the NLC responds with a restoring force upon distortions of the director field. In addition, the orientational order makes the material properties uniaxially anisotropic. The material properties are described by tensors depending on $\boldsymbol{n}$ which will be given in Chapter 2. Since the order parameter depends on the temperature (especially near transition to other phases [25]), the relative anisotropy of the material tensors depends on the temperature as well. For the viscosities and conductivities, an Arrhenius-like temperature dependence is superimposed [28, 29] that is usually much stronger and will be important for comparing the proposed model with experiments (Chapter 5.5).

The NLCs used in the relevant experiments are the standard substance *4-methoxybenzylidene4′-n-butyl-aniline* (MBBA), and the newly introduced material *4-ethyl-2-fluoro-4′-[2-(trans-4-pentylcyclohexyl)-ethyl] biphenyl* (I52). I52 was found to be a good material for EHC experiments [30, 31, 32] with some properties complementary to that of MBBA. MBBA is the only room-temperature nematic with negative dielectric anisotropy where all material parameters have been measured; in I52, some parameters had to be fitted, see Appendix A.1. In the usual prepa-

rations of cells MBBA develops a sufficiently high electric conductivity for EHC [$\approx 10^{-8}(\Omega\mathrm{m})^{-1}$] while I52 must be doped with an ionizable dopant [30].

## The experimental system

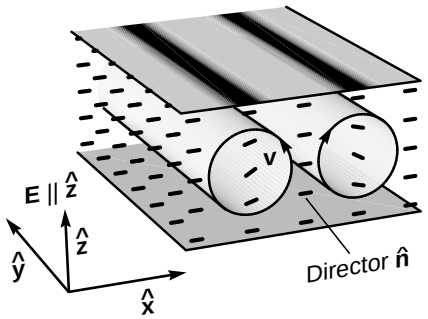


Fig.1.1a: Cell geometry for planar EHC with a section of a roll pattern $\mathbf{v}$ = velocity

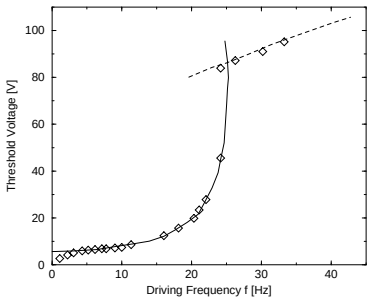


Fig.1.1b: Typical threshold curves for MBBA; — : conductive range, - - - : dielectric range.

The system consists of a nematic liquid crystal with negative or only mildly positive dielectric anisotropy sandwiched between two glass plates with transparent electrodes. When applying an AC voltage (typically, $\overline{V} = 10$V with a frequency of $10 \cdots 1000$ Hz) and increasing the rms $\overline{V}$ above a certain threshold, the non-convecting basic state becomes unstable in favour of a periodic state.

Throughout this work, I consider a planar-homogeneous alignment of the director at the electrodes inducing the anisotropy of the system and defining the $x$ axis, see Fig. 1.1a. A very detailed description of the experimental setup dealing also with the intricacies in making cells of I52, is given in the PhD thesis of M. Dennin [31]; see also [30].

## Patterns

The driving force for EHC is the electric volume force acting on space charges that are generated by initial director distortions together with a positive conductivity anisotropy. This mechanism was suggested by Carr [33] and incorporated into a one-dimensional model by Helfrich [34]. See the Chapters 5.3 and 5.6 for a discussion.

The first experiments of Williams and Kapustin [35, 36] were interpreted to show normal rolls, i.e., the roll axis is perpendicular to the equilibrium alignment of the director. Later on, one observed oblique rolls [37] where the roll axis is tilted with respect to the $y$ direction (Fig. 1.1a).

Most notable are travelling rolls which have been observed as early as 1978 [38]. They were found in a broad parameter range in different NLCs (MBBA, Phase 5,

and I52) by different groups [39, 40, 41, 30, 42] and seem to be generic for relatively thin and clean cells. In most experiments, the bifurcation appears to be continuous (forward), but in very sensitive experiments, one found a small hysteresis [43, 39].

Finally, EHC is the best (and, until recently, the only) system where thermal fluctuations could be observed directly [39, 44]. For an overview of some experiments, see Ref. [40].

## Theoretical description

The one-dimensional model of Helfrich was generalized to include AC driving [45], to two dimensions [46], and finally to a fully three-dimensional treatment [47, 48, 49]. In this work, the standard hydrodynamic description [26, 27, 25] together with the three-dimensional formulation for EHC is referred to as the Standard Model (SM). For a review, see, e.g., [50, 24] or, for the older works, the books of Blinov [28] and Chandrasekhar [51].

The linear analysis in Chapter 5 results in an eigenvalue equation for the growth rate $\lambda(\boldsymbol{q}, R) = \sigma(\boldsymbol{q}, R) \pm i\omega(\boldsymbol{q}, R)$ of periodic perturbations with the wavevector $\boldsymbol{q} = (q_x, q_y)$. The growth rate depends on the primary control parameter $R \propto \overline{V}^2$ describing the external driving and on the AC frequency $\omega_0$. The real part $\sigma$ of one of the eigenvalues crosses zero upon increase of $R$ at fixed $\boldsymbol{q}$ beyond a value $R_0(\boldsymbol{q})$, while the real parts of the other eigenvalues with the same wavevector $\boldsymbol{q}$ remain negative. The neutral surface $R_0(\boldsymbol{q})$ is defined, for any $\boldsymbol{q}$, by the condition that the most unstable mode has a vanishing growth rate, $\sigma(\boldsymbol{q}, R_0) = 0$. Minimizing $R_0(\boldsymbol{q})$ with respect to $\boldsymbol{q}$ gives the threshold $R_c = R_0(\boldsymbol{q}_c)$ with the critical wavevector $\boldsymbol{q}_c$ and the critical frequency (Hopf frequency) $\omega_c = \omega(\boldsymbol{q}_c, R_c)$ of the pattern.

In the SM, $\omega_c$ is always equal to zero indicating a stationary bifurcation (this is of course not accidental, but consitutes a generic case in systems with reflection symmetry). The $z$ and time symmetries of the mode becoming first unstable depends on $\omega_0$. I treat the case of relatively low frequencies, i.e., the so-called conductive range (solid curve in Fig. 1.1b). The modes for higher frequencies are called dielectric modes (dashed in Fig. 1.1b).

In the case of a nonzero $\omega_c$, two degenerate oscillatory modes with frequency $\pm\omega_c$ become unstable simultanously at threshold, which is the definition for a Hopf bifurcation (see, e.g., [10]). The two modes can be identified as the left- and right travelling waves. Even with extreme values of the material parameters and inclusion of flexoelectric terms one never found a Hopf bifurcation as first instability in the SM [52]. This gave rise to develop and explore in this thesis a generalization of the SM, the Weak Electrolyte Model (WEM).